Available online at www.sciencedirect.com

SCIENCE DIRECT®

Thin Solid Films 501 (2006) 299 – 302

thin solid films

www.elsevier.com/locate/tsf

Self-assembled single wall carbon nanotube field effect transistors and AFM tips prepared by hot filament assisted CVD

L. Marty [a], A. Iaia [a], M. Faucher [b], V. Bouchiat [b], C. Naud [a], M. Chaumont [a], T. Fournier [b], A.M. Bonnot [a,*]

[a] LEPES-CNRS, BP166, 38042 Grenoble Cedex 9, France
[b] CRTBT-CNRS, BP166, 38042 Grenoble Cedex 9, France

Available online 26 August 2005

Abstract

The ability of the HFCVD to synthesize SWNTs using cobalt as catalyst has been applied to the preparation of self-assembled single wall carbon nanotube field effect transistor and tips for AFM imaging. This self-assembling batch process fabrication technique has allowed us to fabricate carbon nanotube-based devices that are directly usable without any post-treatment.
© 2005 Published by Elsevier B.V.

Keywords: Carbon nanotubes; CVD; Molecular electronics; Atomic force microscopy

1. Introduction

Single-walled carbon nanotubes (SWNTs) are cylindrical molecules which can be structurally represented by the rolling up of a graphene sheet [1]. Their very high aspect ratio (diameter is typically of the order of 1 nm and length can reach 100 μm), combined with the peculiar properties of graphite confer them extraordinary mechanical and electronic properties. Among them is their ability to be either metallic or semiconducting, depending on curvature and chirality of the rolled graphene plane.

For these reasons, single-walled carbon nanotubes (SWNTs) are very attractive as 1D wires to be used for interconnects in nanoelectronics [2–4]. Moreover, the ability of semiconducting SWNTs to behave as Schottky barriers Field Effect Transistors (FET) [5–8] has opened up the possibility to use them in active electronic devices.

Carbon nanotubes (CNT) have unique properties which make them suitable for probes in an Atomic Force Microscope (AFM) [9]. Their mechanical flexibility, with their nanometer tip radii curvature and high aspect ratio, make them ideal probes for high lateral resolution and deep trench AFM imaging. Moreover, chemically and mechanically robust, CNT AFM probes have also the strong advantage to be stable over prolonged imaging [10] as compared with commercially available, very delicate silicon probes of curvature 5–15 nm.

However, implementation of such devices requires precise positioning of the SWNTs. For FET application, the SWNTs have to be connected to metallic electrode. As tips for AFM, the SWNTs have to be placed at the apex of a Si conventional tip, with a good mechanical contact.

For these reasons, bottom-up and batch process fabrication techniques are needed in order to open the way to practical applications. In this aim, self-assembling fabrication techniques are very promising, even more when concerned with in situ localized growth of SWNTs during the synthesis, which allows direct integration of the devices without any further post-treatments [11–14].

We present here a full self-assembling growth process to fabricate in single-step SWNT-based devices. Application of the technique to the integration of batch-processed NT-FET devices and NT-tips to be used as AFM probes is then demonstrated.

* Corresponding author.
E-mail address: bonnot@grenoble.cnrs.fr (A.M. Bonnot).

0040-6090/$ - see front matter © 2005 Published by Elsevier B.V.
doi:10.1016/j.tsf.2005.07.218

2. Sample preparation and characterizations

Fabrication of the samples involves two steps: the first one for preparing the template, the second one for direct HFCVD growth of the nanotubes. Thereafter, samples are directly characterized without any post-synthesis process.

For FET devices, contacts were patterned on thermally oxidized silicon wafers by evaporation and lift-off of a 30-nm-thick layer of titanium covered with a thin 0.5–2-nm Co catalyst film through a submicron resist mask which was obtained using conventional e-beam lithography.

For the growth of NT tips, commercial Si tips were used and covered with a 2–8-nm-thick Co catalyst layer.

HFCVD was then directly performed. The vapour was composed of methane strongly diluted in hydrogen (5–20 vol.%). During the synthesis, a tungsten filament placed at 1 cm above the substrate holder was heated up to 1900–2100 °C, while controlling the deposition temperature with an additional heater placed in the substrate holder. Typical deposition temperatures were in the 750–850 °C range.

Sample morphology has been characterized by field emission scanning electron microscopy (FESEM).

Characterization of the SWNT structure was undertaken by micro-Raman spectroscopy measurements probing an area of the order of 1 μm^2 and using a 633-nm He–Ne laser radiation.

For transport measurements, a gate-controlled characterization of the self-assembled nanotube circuit was undertaken from room temperature to low temperature (4 K) [8,12]. The gate voltage was applied to the back of the doped Si substrate.

3. Carbon nanotube field effect transistors

Fig. 1 shows SEM images of self-assembled NT-FETs with Ti electrodes covered with a top 3 nm (Fig. 1a) and 0.5 nm (Fig. 1b) Co layer. In Fig. 1a, suspended SWNT bundles connected to face electrodes are clearly observed. However, the roughness of the edges of the electrodes gives rise to parasitic growth of carbon nanotube clumps. Moreover, even though localized on top of the electrodes, the 3-nm-thick Co catalyst layer leads to the growth of numerous bundles extending all around the electrodes.

Optimisation of the lithographic process and decrease of the Co catalyst thickness to 0.5 nm have allowed to lower the SWNT density down to the limit of an isolated SWNT wired to the electrodes (Fig. 1b).

Electronic transport studies were then undertaken without any further processing of the devices. At room temperature, all tested samples show purely Ohmic behaviour with resistance ranging from a few kΩ (Fig. 1a) to a few MΩ (Fig. 1b), depending on the number of SWNTs wired to the electrodes.

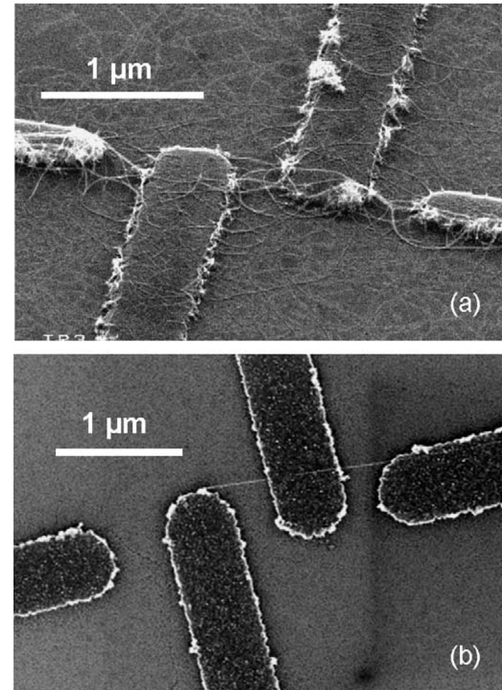

Fig. 1. Scanning electron microscopy image of self-assembled NT-FETs before (a) and after (b) optimisation of the process. In (a), the rough edges of the Ti electrodes with the 3-nm-thick Co top layer lead to the growth of numerous SWNT bundles and a 40-KΩ mean two-point probe resistance. Optimisation of the lithographic process and decrease of the Co layer down to 0.5 nm (b) allowed to wire a single and suspended SWNT bundle to face electrodes with a 2-MΩ resistance.

Fig. 2 shows the dependence at room temperature of the drain-source current I_{ds} on the drain-source voltage V_{ds} and for different back-gate voltage V_{BG}.

Decreasing the gate voltage from positive towards negative values induces the lowering of the resistance of the device which is characteristic of a FET behaviour. In Fig. 2, the field effect between V_{BG}=+30 V and −30 V has divided the resistance by a factor of 100.

The quality of the samples has been characterized by Raman spectroscopy. Fig. 3 shows typical Raman spectrum of our NT-FET. The Raman spectra evidence SWNT tangential Raman lines ω_T between 1550 and 1600 cm^{-1} [15]. The weak signal at ω_D=1325 cm^{-1} originating from disordered graphite points out the good crystallinity of the samples.

The Raman spectrum in Fig. 3a corresponds to a NT-FET with a 100 kΩ two-point resistance. The strong Raman resonant Stokes and anti-Stokes Radial Breathing Modes (RBM) peaks at ±193 cm^{-1} with the broad tangential band around 1525 cm^{-1} are the signature of metallic SWNTs [15]. Moreover, narrow tangential peaks at 1595 cm^{-1} and 1568 cm^{-1} correspond to semiconducting SWNTs. These characteristics confirm the presence of SWNTs with different diameters.

On the contrary, in Fig. 3b, the low intensity and the narrowness of the tangential Raman peaks at ω_T=1593,

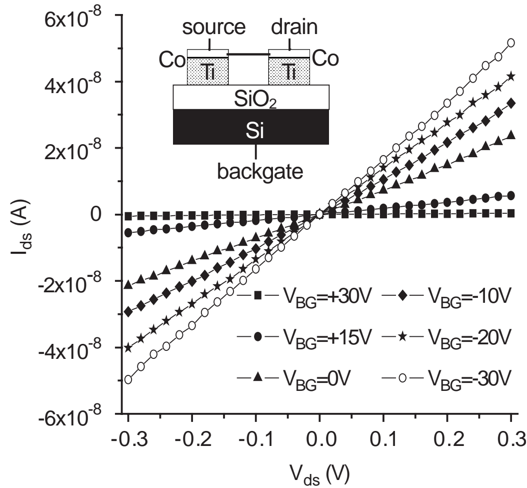

Fig. 2. Room temperature drain-source $I_{ds}-V_{ds}$ curves of a self-assembled CN-FET for different back-gate voltages V_{BG} (decreasing V_{BG} from +30 V to −30 V causes a resistance decrease from 746 MΩ to 6 MΩ).

1581, 1570 cm^{-1} with the absence of any RBM signal suggest the presence of very few semiconducting SWNTs. In this case, the two-point resistance is of the order of 2 MΩ. By the way, the lower the SWNT density, the weaker the Raman intensity of the tangential modes and the higher the circuit resistance.

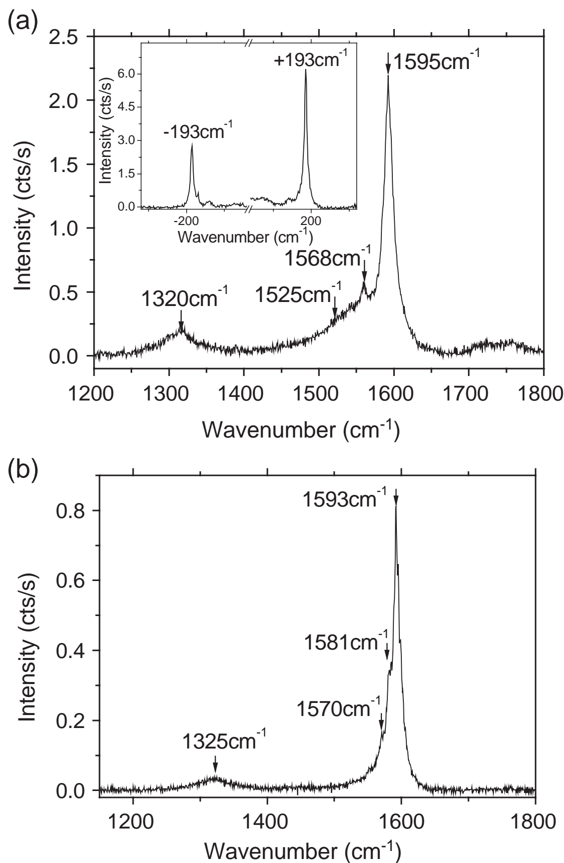

Fig. 3. Raman spectra of NT-FET with two-point probe resistance of 100 KΩ (a) and 2 MΩ (b).

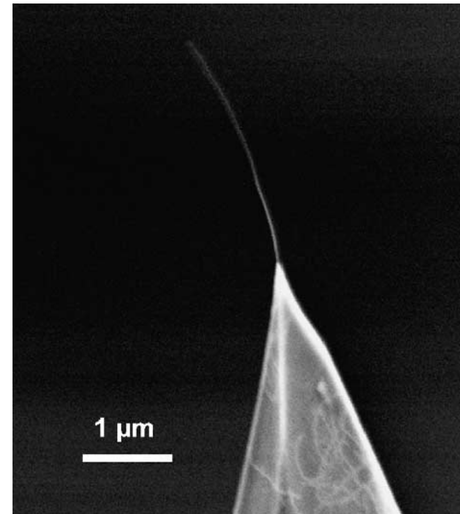

Fig. 4. HFCVD self-assembled growth of NT-tip on conventional Si tip for AFM imaging.

4. Carbon nanotube AFM tips

HFCVD deposition of SWNTs on commercial Si tips (NT-tip) were undertaken using same conditions as for self-assembled NT-FET, except the cobalt catalyst thickness which appeared to be the critical parameter. Cobalt layer thickness superior to 9 nm led to the growth of too many nanotubes at the tip apex, while for too thin one (≤4 nm), the yield of SWNT growth at the apex of the Si tip becomes negligible. With an optimal catalyst thickness of the order of 5–8 nm, the yield of production of a unique SWNT bundle at the apex of a commercial Si tip is of about 20–30%.

Fig. 4 shows a self-assembled NT-tip grown on a Si probe covered with an 8-nm-thick Co layer.

The exceptional advantage of the method appears to be the growth of a unique bundle extending from the apex of the Si tip, while parasitic bundles grown along the Si tip sides are stuck by van der Waals interaction. However, there are still crucial problems to be solved. One of them concerns the control of the NT length, which at present varies from a few hundred of nm to a few μm.

5. Conclusion

The ability of the HFCVD technique to prepare self-assembled SWNT-based devices using cobalt as catalyst has been demonstrated.

For electronic application, the strong advantage of the method is the growth of suspended SWNTs which are self-wired during the synthesis. Electronic transport measurements are then directly undertaken after the growth, without

any further post treatment. In particular, the optimisation of both the cobalt catalyst thickness and the synthesis parameters has led to the wiring of a unique suspended SWNT to Ti electrodes.

The same self-assembling method has been successfully applied to the growth of a SWNT bundle at the apex of commercial Si tips.

The strong advantage of the method appears to be its compatibility with bottom-up large-scale fabrication of batch processed carbon nanotube-based devices.

References

[1] R. Saito, G. Dresselhaus, M.S. Dresselhaus, Physical Properties of Carbon Nanotubes, Imperial College Press, 1998.
[2] C. Dekker, Carbon nanotubes as molecular quantum wires, Phys. Today (1999 May) 22.
[3] M.S. Dresselhaus, G. Dresselhaus, Ph. Avouris (Eds.), Carbon Nanotubes, Synthesis, Structure, Properties and Applications, Topics in Applied Physics, Springer-Verlag, 2001, For a review see.
[4] H. Dai, Surf. Sci. 500 (2002) 218.
[5] S.J. Tans, M.H. Devoret, H. Dai, A. Thess, R.E. Smalley, L.J. Geerligs, C. Dekker, Nature 286 (1997) 474.
[6] A. Bachtold, P. Hadley, T. Nakanishi, C. Dekker, Science 294 (2001) 1317.
[7] S. Heinze, J. Tersoff, R. Martel, V. Derycke, J. Appenzeller, P. Avouris, Phys. Rev. Lett. 89 (2002) 106801.
[8] L. Marty, V. Bouchiat, A.M. Bonnot, M. Chaumont, T. Fournier, S. Decossas, S. Roche, Microelectron. Eng. 61–62 (2002) 485.
[9] Y. Nakayama, S. Akita, New J. Phys. 5 (2003) 128.1.
[10] T. Larsen, K. Moloni, F. Flack, M.A. Eriksson, M.G. Lagally, Appl. Phys. Lett. 80 (2002) 1996.
[11] N.R. Franklin, Y. Li, R.J. Chen, A. Javey, H. Dai, Appl. Phys. Lett. 79 (2001) 4571.
[12] L. Marty, V. Bouchiat, C. Naud, M. Chaumont, T. Fournier, A.M. Bonnot, Nanoletters 3 (2003) 1115.
[13] E. Yenilmez, Q. Wang, R.J. Chen, D. Wang, H. Dai, Appl. Phys. Lett. 80 (2002) 2225.
[14] Q. Ye, A.M. Cassel, H. Liu, K.J. Chao, J. Han, M. Meyyappan, Nanol. 4 (2004) 1301.
[15] M.S. Dresselhaus, P.C. Eklund, Adv. Phys. 49 (2000) 705.